

### Central European Journal of Chemistry

# Investigation on the catalytic activity of doped low-percentage oxide catalysts Mn/ZnO obtained from oxalate precursor

Research article

Borjana V. Donkova<sup>1\*</sup>, Katja I. Milenova<sup>2</sup>, Dimitar R. Mehandjiev<sup>2</sup>

#### Received 26 July 2007; Accepted 21 November 2007

**Abstract:** The precursors with a low manganese content ≤ 0.07% Mn were synthesized by spontaneous crystallization from Zn<sup>2+</sup>, Mn<sup>2+</sup> and  $C_2O_4^{2}$  - containing solutions. The initial ratio  $Zn^{2}+C_2O_4^{2}=1:1$  and 1:2 influences the morphology and prevailing orientations of the crystallites in the oxalate samples. The presence of such small Mn content in the samples does not change the morphology or size of the crystals. The ZnO and Mn/ZnO oxides with manganese content from 0.51×10-2 to 15.1×10-2 Wt % are obtained after thermal decomposition of the oxalates. The oxides preserved the morphology of the precursors. The catalytic tests show that the pure ZnO has a poor activity for CO oxidation reaction. Its doping with Mn promotes the catalytic activity (up from twice to five times) in spite of the very low contents of the dopants. The observed increase of the activity depends on both dopant concentration and Zn<sup>2+</sup>:C<sub>2</sub>O<sub>2</sub><sup>2</sup>-ratio, probably due to the different mechanism of the manganese inclusion and different morphology of the oxides. The catalysts of the 1:2 series are more active in CO oxidation reaction.

**Keywords:** ZnO • ZnC<sub>2</sub>O<sub>4</sub>:2H<sub>2</sub>O • Manganese • Cocrystallization • CO oxidation

© Versita Warsaw and Springer-Verlag Berlin Heidelberg.

### 1. Introduction

The scientists' interest in ZnO is determined by its specific electrical, optical and structural properties, as well as by the possibility to modify them additionally by doping or changing the particle size and morphology. The various applications of ZnO in such technics and in contemporary technologies are discussed in Ref. [1-5]. The use of the slightly soluble ZnC<sub>2</sub>O<sub>4</sub>·2H<sub>2</sub>O as a precursor for preparing nano-sized pure ZnO and ZnO, doped with transition metals' ions has been growing in the last few years [6-16]. Advantages of the oxalate precursor are its easy synthesis, low temperature of decomposition and the evolution of a large amount of volatile substances (CO, CO<sub>2</sub>, H<sub>2</sub>O), which is prerequisite for the formation of the oxide with high surface area value. The microstructure and the morphology of the

precursor and the oxide produced can be modified by changing the synthesis procedure [6-13]. Another advantage is that the oxalates from the magnesium series (Mg, Mn, Co, Fe, Ni and Zn) are isomorphous. This enables modification of the ZnO physical properties by doping of the precursor in the course of its synthesis [14-16]. The latter approach has been widely applied recently to obtain new generation of microelectronic devices and magneto-optic components.

In addition to the changes in the ZnO physical properties, the ions of Mn, Co, Ni and Cu can also influence its catalytic properties since the oxides of these metals in the bulk phase or deposited on a support are active catalysts in reactions of complete oxidation. The catalytic properties of pure and doped ZnO in the reaction of CO oxidation have not been studied in detail, except for some old publications [17-20] (the dopants

<sup>&</sup>lt;sup>1</sup> Department of Inorganic Chemistry, Faculty of Chemistry, University of Sofia, 1 J. Bouchier Av., Sofia 1164, Bulgaria

<sup>&</sup>lt;sup>2</sup> Institute of General and Inorganic Chemistry, Bulgarian Academy of Sciences, Acad. G. Bonchev Str., bl 11, Sofia 1113, Bulgaria

<sup>\*</sup> E-mail: nhbd@inorg.chem.uni-sofia.bg

are Li, Ga, In, TI in these cases). This is probably due to its poor catalytic activity. Our expectation is that the intercalation of isomorphous admixtures as 3d-metal ions in the precursor's crystal lattice would lead to their more uniform distribution in the oxide support resulting in promoted catalytic activity in the oxidation reactions.

Our previous investigations on the mechanism of cocrystallizationofMn,Co,NiandCuinZnC,O,·2H,Ocrystals [21-23] have shown that the different concentrations of the oxalate ions in the initial system determine both a different amount of included admixture and a different mechanism of their inclusion. Therefore the synthesis of the Zn-Mn precursor, studied in the present work, was carried out under conditions, analogous to those used in [21] – from solutions of ZnSO<sub>4</sub> and K<sub>2</sub>C<sub>2</sub>O<sub>4</sub> at initial ratio  $Zn^{2+}$ : $C_2O_4^{2-}$  = 1:1 and 1:2. The admixture, included in the precursor by different mechanisms, would in different ways affect the activity of the support. On the other hand it is known, that during the course of synthesis of 3d-oxalates, different concentrations of oxalate ions affects [24-26] the processes of nucleation, crystal growth, the form and average size of particles, their size distribution and also their degree of agglomeration. The latter fact has been confirmed also in the Ref. [7], where alcoholic solutions were used. For this reason the solid phase product, obtained by thermal decomposition of the oxalate, will possess characteristic morphological and microstructural features and this is among the most important factors, influencing the catalytic activity.

The present study aims to establish both the applicability of the sparingly soluble oxalates, doped by co-crystallization with Mn<sup>2+</sup> as precursors for preparing active lightly doped catalysts and also the influence of the mechanism of dopant inclusion in the precursor on its catalytic activity. The oxidation of CO has been selected as a model reaction.

# 2. Experimental

#### 2.1. Synthesis of the samples

The samples of pure and manganese doped  $ZnC_2O_4$ : $ZH_2O$  were synthesized by spontaneous crystallization, wherein the initial solutions had two different ratios of zinc and oxalate ions. Samples having a ratio  $Zn^{2+}$ : $C_2O_4^{2-}$ =1:2 were prepared and denoted as the (1:2) series while the second ratio  $Zn^{2+}$ : $C_2O_4^{2-}$ =1:1, was denoted as the (1:1) series. Four samples were obtained in each series – three of them doped with manganese and one without doping i.e. a pure zinc oxalate sample.

The initial reagents were of high purity grade

ZnSO<sub>4</sub>·7H<sub>2</sub>O, K<sub>2</sub>C<sub>2</sub>O<sub>4</sub>·H<sub>2</sub>O and MnSO<sub>4</sub>·5H<sub>2</sub>O. The experimental conditions were T = 25.0 ± 0.5°C, initial acidity of the system pH = 3.0 ± 0.1, rate of electromechanical stirring 1000 rpm, and two different ratios of Zn<sup>2+</sup>:C<sub>2</sub>O<sub>4</sub><sup>2-</sup>. The acidity was chosen so as to avoid hydrolysis processes, to stabilize the divalent state of manganese, and as well as to eliminate the strong dependence of the solubility of the ZnC<sub>2</sub>O<sub>4</sub>·2H<sub>2</sub>O on pH of the medium in more acidic solutions [27]. Concentrated initial solutions had to be used since the purpose was to obtain finely crystalline zinc oxalate precursor. For the series (1:2) the concentrations were 0.45 M ZnSO<sub>4</sub> and 0.9 M K<sub>2</sub>C<sub>2</sub>O<sub>4</sub>, while for the (1:1) series the two solutions were equimolar - 0.45 mol/dm3. For these highly concentrated solutions the supersaturation coefficient S was evaluated as  $S = \sqrt{IP/K_{sp}}$ , where IP is the ionic solubility product and  $K_{so}$  is the thermodynamic solubility product. In both the series the supersaturation corresponds to the region of homogeneous nucleiformation of ZnC<sub>2</sub>O<sub>4</sub>·2H<sub>2</sub>O [28,29].

The spontaneous crystallization of ZnC2O4·2H2O was carried out as a two-flow precipitation technique, which leads to the best defined supersaturation in the case of slightly soluble substances. Equal volumes (0.150 cm<sup>3</sup>) of the initial ZnSO<sub>4</sub> and K<sub>2</sub>C<sub>2</sub>O<sub>4</sub> solutions were poured simultaneously from two opposite ends of the reaction vessel upon continuous stirring. At a specific time point from the beginning of the process, which is different for the two series (40 s for 1:1) and (80 s for 1:2), the reaction system was diluted with bidistilled water at a ratio 1:1. This was done with the aim of decreasing the supersaturation so to prevent the growing of the finely formed crystalline phase. The duration of the synthesis with incessant stirring was 10 days. During this period the samples were undergoing a process of recrystallization, while in the case of the doped samples, a process of the dopant redistribution was also occurring. The white precipitate obtained was filtered and after washing it twice it was suspended in water and submitted to ultrasound treatment. Thereafter it was filtered, washed again and dried in air.

For the preparation of the doped samples, different amounts of the dopant (taken from the  $0.25 \text{ M MnSO}_4$  stock solution) were added to the  $\text{K}_2\text{C}_2\text{O}_4$  solution before the mixing step. This amount was the same for both the series (1:1) and (1:2).

In order to prepare pure and manganese doped ZnO the synthesized oxalate precursors were calcined for 1 h in air at 470°C, then tempered in a dessicator and weighed. For the sake of comparison one of the samples was calcined for 3 hours. The oxalate decomposition was controlled by accounting for the changes in the weight of the sample.

The so prepared samples are denoted by "Wt%-Mn/  $ZnC_2O_4\cdot 2H_2O$  (1:2)" or (1:1) for the oxalate precursors and with "Wt%-Mn/ZnO (1:2)" or (1:1) for the oxides, respectively. The labeling (1:2) or (1:1) shows the initial ratio  $Zn^{2+}:C_2O_4^{-2-}$  while the index "Wt %" shows the content of Mn in weight percentage.

#### 2.2. Sample characterization

The X-ray diffraction (XRD) analysis was carried out on a Siemens powder diffractometer model D500 using CuK $\alpha$  radiation in a 2 $\theta$  diffraction interval of 10-60 degrees. The identification of the phases was done by means of the database JCPDS – International Center for Powder Diffraction Data.

Diffraction data were processed using the Powder Cell program [30]. The average coherent domain size was estimated from the angular dependence of FWHM's of all recorder diffraction lines.

The determination of the specific surface area and the characterization of the porous texture of the samples was carried out by nitrogen adsorption at the boiling temperature of liquid nitrogen (77.4 K) using a conventional volume-measuring apparatus. Before the measurements were taken, the samples were degassed at 423K until the residual pressure became lower than 1.333x10<sup>-2</sup> Pa.

The nitrogen  $(N_2)$  and the krypton (Kr) adsorption-desorption isotherms were used to calculate the specific surface area  $(A_{\rm BET})$  using the BET equation. The total pore volume  $(V_{0.95})$  was estimated based on the adsorbed amount at a relative pressure of 0.95. The size distribution of the mesopores was evaluated by the method of Pierce [31] using the adsorption branches of the isotherms.

The X-ray photoelectron spectroscopy (XPS) studies were performed in a VG Escalab II electron spectrometer using AlK $\alpha$  radiation with energy of 1486.6 eV. The residual gas pressure in the analysis chamber was  $10^{-7}$  Pa. The scanning electron microscope (SEM) observation was carried out on a JEOL JSM-5510 apparatus. The method of depositing a golden coating was applied using a JFC-1200 device. The electron paramagnetic resonance (EPR) spectra were registered as a first derivative of the absorption signal in the temperature interval 100-400 K using an ERS 220/Q instrument.

#### 2.3. Catalytic investigation

The catalytic activity of the samples was studied in an isothermal plug flow reactor enabling operation under steady-state conditions without temperature gradients. The size of the catalyst particles (0.3-0.6 mm) was

chosen taking into account the reactor diameter (6.0 mm) and the hourly space velocity (20 000 h-1) in order to reduce the effect of the pore diffusion. The gas feed flow rate was 4.4 l/h, the catalyst bed volume was 0.2 cm³ and the mass of the catalyst charge was 0.5-0.6 g. The catalytic oxidation of CO was performed at the temperature interval 200 – 400°C, the oxidizing agent used being oxygen from the air (gas mixture: 21%  $\rm O_2$  and 79%  $\rm N_2$ ). The preliminary treatment of the catalyst included heating in air flow at 120°C for 1 hour. The flow of CO was fed into the reactor by an Ismatex M62/6 pump (Switzerland).

The initial concentration of carbon monoxide was 0.5 vol. %. The carrier gas was air (a mixture of 21%  $O_2$  and 79%  $N_2$ ). A Maihak ( $O_2$ /CO/CO $_2$ ) gas analyser was used to measure the CO and CO $_2$  concentrations with an accuracy of  $\pm 0.1$  ppm, while the oxygen measurement accuracy was  $\pm 100$  ppm.

Table 1. Composition of weight (Wt, %) and molar (N, %) percentages and specific surface area (A<sub>BET</sub>) of the obtained precursors.

Samples	Manganese content		A <sub>BET</sub> , m²/g
	Wt, %	N, %	
0.005 Mn/ZnC <sub>2</sub> O <sub>4</sub> ·2H <sub>2</sub> O (1:2)	0.0049	0.0169	1.3
0.017 Mn/ZnC <sub>2</sub> O <sub>4</sub> ·2H <sub>2</sub> O (1:2)	0.0169	0.0583	1.0
0.067 Mn/ZnC <sub>2</sub> O <sub>4</sub> ·2H <sub>2</sub> O (1:2)	0.0667	0.2300	1.6
0.002 Mn/ZnC <sub>2</sub> O <sub>4</sub> ·2H <sub>2</sub> O (1:1)	0.0022	0.0076	1.6
0.016 Mn/ZnC <sub>2</sub> O <sub>4</sub> ·2H <sub>2</sub> O (1:1)	0.0155	0.0534	2.0
0.021 Mn/ZnC <sub>2</sub> O <sub>4</sub> ·2H <sub>2</sub> O (1:1)	0.0206	0.0710	2.0
$ZnC_2O_4 \cdot 2H_2O$ (1:2)	-	-	1.4
$ZnC_2O_4 \cdot 2H_2O$ (1:1)	-	-	2.0

### 3. Results and discussion

### 3.1. Precursors (Mn/ZnC<sub>2</sub>O<sub>4</sub>·2H<sub>2</sub>O)

The data on the composition and specific surface areas of the obtained samples of pure and doped zinc oxalate are shown in Table 1. The results show that precursors with a low manganese content  $\leq 0.07\%$  Mn are obtained. As it could be expected in view of the previous investigations on the mechanism of co-crystallization of Mn in ZnC $_2$ O $_4\cdot$ 2H $_2$ O the amount of included dopant depends on the ratio of Zn $^{2+}$ :C $_2$ O $_4^{2-}$ , in spite of the fact that the applied initial concentrations of the admixture ions are the same for both the series [21]. The excess of oxalate ions in case of the (1:2) series leads to inclusion of a higher amount of manganese. The specific surface area of the precursors, determined by the BET method, is not high - 1 up to 2 m $^2$ /g. In the frame of experimental error (3%) there is a tendency, although weakly

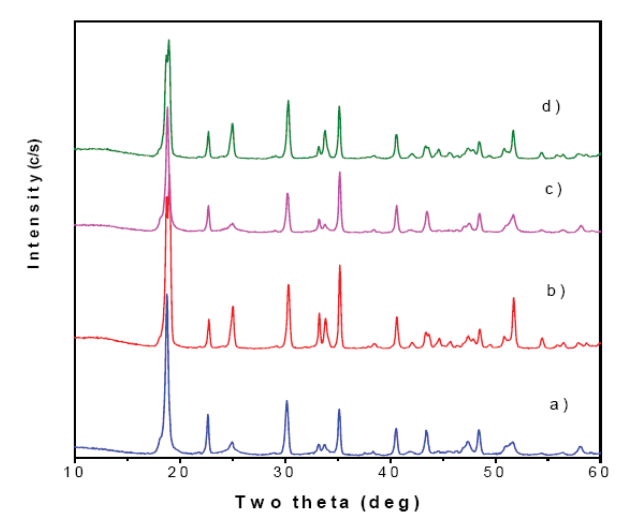


Figure 1. X-ray diffractograms of a) ZnC<sub>2</sub>O<sub>4</sub>·2H<sub>2</sub>O (1:1); b) ZnC<sub>2</sub>O<sub>4</sub>·2H<sub>2</sub>O (1:2); c) 0.021 Mn/ZnC<sub>2</sub>O<sub>4</sub>·2H<sub>2</sub>O (1:1); d) 0.067 Mn/ZnC<sub>2</sub>O<sub>4</sub>·2H<sub>2</sub>O (1:2).

expressed, that the samples of the (1:1) series possess a higher specific surface area.

The X-ray diffraction studies are shown in Fig. 1. The figure represents pure oxalates from series (1:1) and (1:2) and only those samples of the two groups that contain the largest manganese amount in the respective series (Fig. 1c and d). The results show the formation of monoclinic  $ZnC_2O_4 \cdot 2H_2O$  (JCPDS 25-1029) in both series; however the intensities of the peaks vary depending on the  $Zn^{2+}:C_2O_4^{2-}$  ratio in the initial solutions. This variation is due to differences in the crystallinity of the samples.  $ZnC_2O_4 \cdot 2H_2O$  (1:2) is more crystalline than  $ZnC_2O_4 \cdot 2H_2O$  (1:1). As a consequence is the splitting of the strongest peak of the sample, synthesized at ratio 1:2. The observed differences are displayed also in the case of doped samples (Fig. 1c and d).

In our opinion the dependence of the peaks' intensity on  $C_2O_4^{\ 2^-}$  concentration is connected to the supersaturation, created in both systems which determines the different conditions of crystallization. The supersaturation coefficient S amounts to 1936 for the series (1:2), while it is 1369 for the series (1:1). The synthesis in both cases corresponds to the region of homogeneous nucleus formation [28,29], but the different

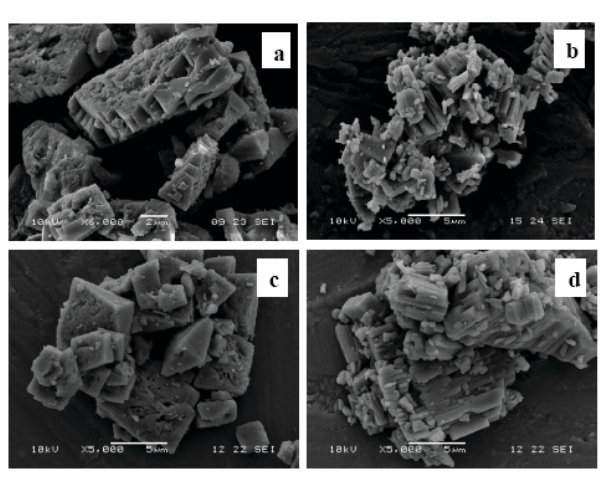


Figure 2. Electron micrographs of a) ZnC<sub>2</sub>O<sub>4</sub>·2H<sub>2</sub>O (1:1); b) ZnC<sub>2</sub>O<sub>4</sub>·2H<sub>2</sub>O (1:2); c) 0.021 Mn/ZnC<sub>2</sub>O<sub>4</sub>·2H<sub>2</sub>O (1:1); d) 0.067 Mn/ZnC<sub>2</sub>O<sub>2</sub>·2H<sub>2</sub>O (1:2).

degree of supersaturation will influence the type of initial formed precipitate, mechanism of crystal growth, size and shape of the crystals because of changes in the specific surface energy.

The electron micrographs shown in Fig. 2 illustrate the above statement. The samples, obtained from equimolar initial solutions (Fig. 2a, 2c), contain characteristic octahedral crystals. In the samples, obtained with excess of the oxalate ions (Fig. 2b, 2d), the prevailing number of crystals has a prismatic form and they form aggregates.

The parameters of the crystal lattice, evaluated by the least square method on the basis of the X-ray diffractograms, are given in Table 2 with those of a standard (JCPDS 25-1029). The mean size of the crystallites is also listed. The obtained values show that the excess of oxalate ions (1:2 series) results in higher values of the angle  $\beta$  and the parameters  $\boldsymbol{b}$  and  $\boldsymbol{c}$  in the cases of both pure zinc oxalate and Mn doped sample. A tendency is observed to obtain larger size crystallites in the (1:2) series samples, which is in agreement with their lower specific surface areas (Table 1). Due to the low concentration of Mn in the samples (0.021% and 0.067%) we cannot draw a conclusion in regard to its influence on the crystal lattice parameters.

Table 2. Parameters of the crystal lattice and crystallites size of the precursors, shown in Fig. 1.

Samples	Lattice constan	Lattice constants a,b,c (Å) and β (degr)			Size, nm
	a ± 0.002	$b \pm 0.002$	c ± 0.002	$\beta$ $\pm$ 0.15	
Ref. JCPDS 25-1029	11.804	5.403	9.921	127.70	
ZnC <sub>2</sub> O <sub>4</sub> ·2H <sub>2</sub> O (1:1)	11.818	5.388	9.829	127.22	29
ZnC <sub>2</sub> O <sub>4</sub> ·2H <sub>2</sub> O (1:2)	11.816	5.402	9.898	127.72	39
0.021Mn/ZnC <sub>2</sub> O <sub>4</sub> ·2H <sub>2</sub> O (1:1)	11.816	5.387	9.838	127.24	30
0.067Mn/ZnC <sub>2</sub> O <sub>4</sub> ·2H <sub>2</sub> O (1:2)	11.811	5.401	9.899	127.62	36

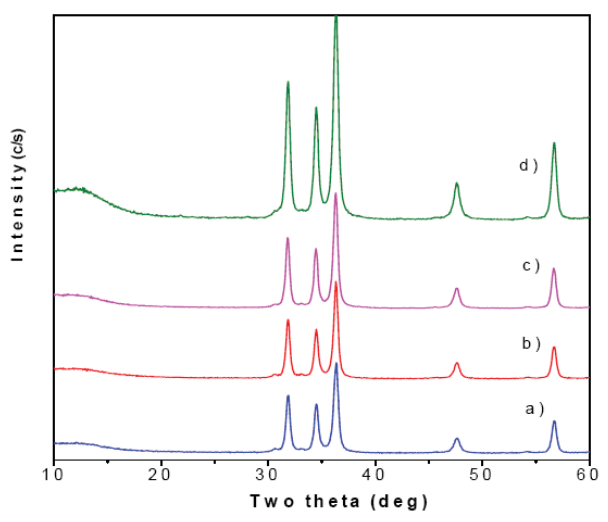


Figure 3. X-ray diffractograms of a) ZnO (1:1); b) ZnO (1:2); c)0.047 Mn/ZnO (1:1); d) 0.151 Mn/ZnO (1:2).

#### 3.2. Oxide catalysts (Mn/ZnO)

The composition and the specific surface areas ( $A_{\rm BET}$ ) of the pure and Mn-doped oxide samples are represented in Table 3. The mass loss after thermal treatment at 470°C is about 56-57%, corresponding to the oxalate transformation into oxide. Although after the calcination the dopant amount becomes more than twice higher, its concentration remains extremely low in view of the standard concept for an active component in catalysis. Table 3 illustrates that the specific surface areas of all the oxides are almost the same within the experimental error but are considerably higher with respect to that of the precursors.

The observed increase in the value of  $A_{\text{BET}}$  is expected, as one of the reasons for selecting an oxalate precursor was the liberation of a considerable amount of gases during the thermal decomposition, which causes increase in the surface area of the final product. Moreover, a detailed study of the early stage of the growth of nanoscale zinc oxide crystallites [32] showed that in the case of the oxalate precursor there occurred no particle agglomeration processes at temperatures up to 470°C. The surface area obtained in our study is comparable to that obtained by other authors after decomposition in air - 25 m<sup>2</sup>/g, 18 m<sup>2</sup>/g [33,34]. In view of studying the influence of the calcination duration on the sintering of the samples one of them was calcined for 3 hours instead of 1 hour. The results show that there was no difference in the specific surface area.

The X-ray diffraction analysis of the oxide samples (Fig. 3) illustrates the formation of wurtzite ZnO (JCPDS 36-1451) in both series. The results for (1:2) and (1:1) are identical, in contrast to the observed in Ref. [7]. However, the electron micrographs (Fig. 4) show that

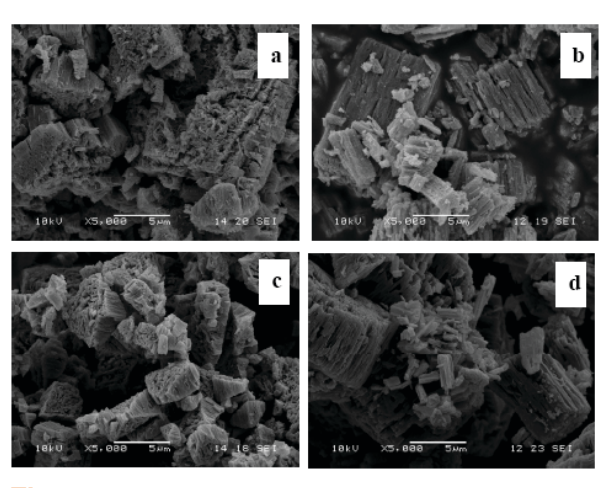


Figure 4. Electron micrographs of a) ZnO (1:1); b) ZnO (1:2); c) 0.047 Mn/ZnO (1:1); d) 0.151 Mn/ZnO (1:2).

the difference in the morphology between series (1:2) and (1:1) is preserved. This fact points to the presence of an orientational similarity between the oxides and their precursors, which is most probably due to a topotactic transformation process. A similar morphological correspondence has been discussed in the papers [9,11,32], whereupon in Ref.[32] the authors introduce the term "memory effect". In addition to the topotactic correspondence the micrographs in Fig. 4 show that the gases being liberated during the dehydration process diffuse through the crystals in a different way, thus forming different types of channels. A multitude of channels, located between the separate prismatic crystals is observed in the samples (1:2) (Fig. 4b, 4d), while in the case of samples (1:1) (Fig. 4a, 4c) pores and cracks on the surface of the octahedral are observed. Except this in all oxide samples a small fraction of the crystals like those in Fig. 5 can be seen. This observation suggests that the micron-sized crystals are obtained as a result of the growth of nanometer-sized particles.

The parameters of the crystal lattice of the oxides, shown in Fig. 3 are compared in Table 4 with those of a standard (JCPDS 36-1451). The size of the crystallites, determined by XRD, is also listed. Comparison with the crystallite sizes determined using the specific surface area reveals a very good correspondence. With a specific surface area 27 m<sup>2</sup>/g, the size is about 20 nm. With oxalate samples, however, there is a great difference because the crystallite size according to XRD depends on the crystallite imperfectness but during the 10 days of precursor synthesis the internal and external crystal surfaces are perfectioned and the internal defects become inaccessible to gas adsorption. Thus, the external dimensions mainly are determined by the BET method, and they are expected to be close in size to the dimensions visible on electron microscope

**Table 3.** Composition of weight (Wt, %) and molar (N,%) percentages, specific surface area (A<sub>BET</sub>) and total pore volume (V<sub>0.95</sub>) of the pure zinc oxide and Mn-doped oxide.

Samples	Manganese content		A <sub>BET</sub> , m <sup>2</sup> /g	V <sub>0.95</sub> , cm3/g
	Wt, %	N, %		
0.011 Mn/ZnO (1:2)	0.0111	0.0164	25.2	0.041
0,039 Mn/ZnO (1:2)	0.0385	0.0570	25.3	0.038
0.151 Mn/ZnO (1:2)	0.1511	0.2249	26.4	0.040
0.005 Mn/ZnO (1:1)	0.0051	0.0076	24.4	0.038
0.035 Mn/ZnO (1:1)	0.0353	0.0523	25.3	0.041
0.047 Mn/ZnO (1:1)	0.0470	0.0698	25.3	0.038
ZnO (1:2)	-	-	27.4	0.038
ZnO (1:1)	-	-	27.4	0.042

**Table 4.** Parameters of the crystal lattice and crystallites size of the precursors, shown in Fig. 3.

Samples	Lattice constants a,c (Å)		Size, nm
	a ± 0.002	c ± 0.002	
Ref. JCPDS 36-1451	3.249	5.206	
ZnO (1:1)	3.2484	5.2068	19
ZnO (1:2)	3.2491	5.2069	20
0.047 Mn/ZnO (1:1)	3.2478	5.2060	19
0.151 Mn/ZnO (1:2)	3.2481	5.2075	18

#### pictures.

The adsorption-desorption isotherms of the pure and doped ZnO samples of series (1:2) and (1:1) are shown in Fig. 6. For comparison the represented doped oxides contain equal manganese quantities. The other Mn/ZnO samples show isotherms of the same type therefore they are not presented. As it is seen from Fig. 6 the character of ZnO and Mn/ZnO adsorption isotherms is the same. They belong to the type IV isotherms with a hysteresis loop H1, following the nomenclature of IUPAC [35]. This type of hysteresis curves is obtained when the space of the pores is formed by particles close in size, building up aggregates.

The normalized pore size distribution curves, represented in Fig. 7, were plotted on the basis of the adsorption isotherms. It can be observed that: i) there is no substantial difference between the samples of the two series, and ii) the presence of a dopant does not substantially affect this distribution. In all distribution curves there is a maximum in the region 20-30 Å. In the doped samples of the series (1:1) the pore size distribution is located in a narrow range, while in the series (1:2) there is a widening of the curves and appearance of pores with larger diameters.

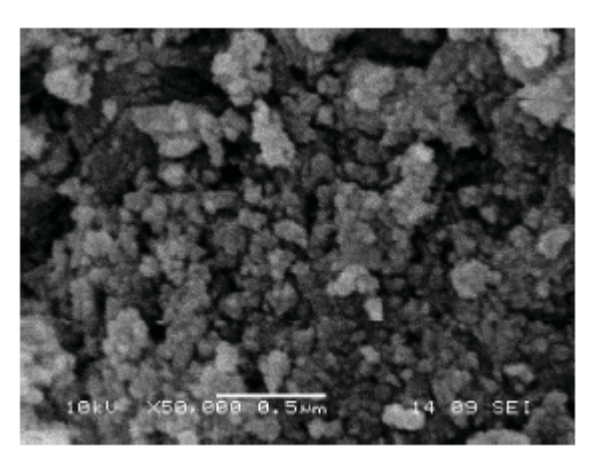
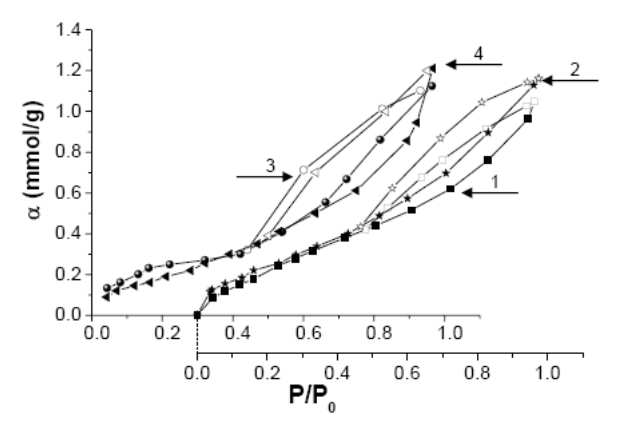


Figure 5. Electron micrograph of the crystals fraction, typical for all oxide samples.



**Figure 6.** Nitrogen adsorption/desorption isotherms at 77.4 K on the samples studied. 1 – ZnO (1:2); 2- ZnO (1:1); 3 - 0.035 Mn/ZnO (1:1); 4 – 0.039 Mn/ZnO (1:2). (Open symbols correspond to desorption; filled symbols correspond to adsorption.)

#### 3.3. Catalytic activity

The results from the catalytic tests in the CO oxidation reaction are grouped with respect to the series and represented in Fig. 8A and 8B.  $I_s$  is the converted amount of CO by 1 m<sup>2</sup> of the surface at a constant space velocity, while T is the temperature in degrees Celsius.

It is seen that in both series the ZnO catalytic activity is changed after doping, although the Mn content is extremely low. The effective purification, accomplished by 1 m² of surface is promoted twice (series 1:1) up to 5 times (series 1:2) at 340°C. Another interesting result is that the catalytic activity depends on the method of preparing the precursor, to be more specific on the ratio Zn²+:C₂O₄²-. The doped catalysts of the 1:2 series are slightly more active than those of the 1:1 series, at one and the same specific surface area and quite close Mn content. Within the framework of a given series no differences in activity are observed in Mn content lower or equal to 0.047%, but the sample containing 0.151% Mn is already more active than the other two samples

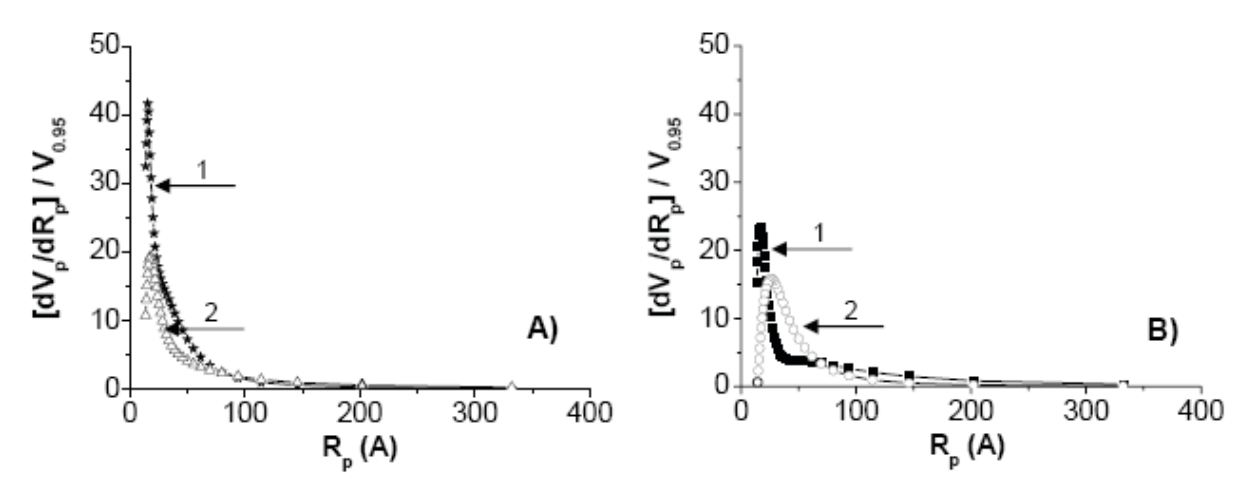


Figure 7. Normalized size distributions of the pores: A) 1- ZnO (1:1); 2- ZnO (1:2); B) 1- 0.035 Mn/ZnO (1:1); 2- 0.039 Mn/ZnO (1:2).

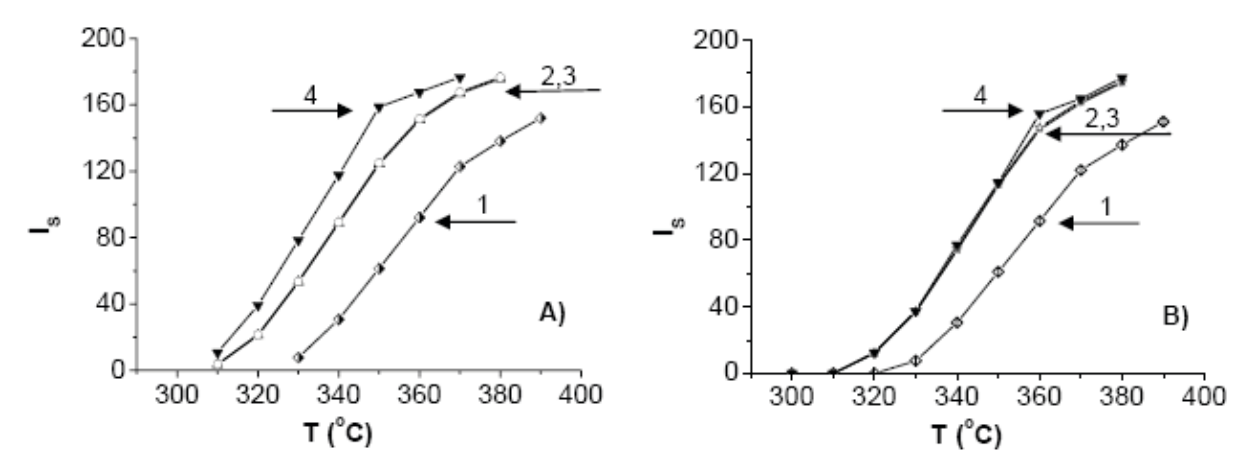


Figure 8. Amount of CO transformed to CO<sub>2</sub> per unit surface area of the catalyst for one hour: A) Series (1:2): 1- ZnO (1:2); 2- 0.039 Mn/ZnO (1:2); 3- 0.011 Mn/ZnO (1:2); 4- 0.151 Mn/ZnO (1:2); B) Series (1:1): 1- ZnO (1:1); 2- 0.035 Mn/ZnO (1:1); 3- 0.005 Mn/ZnO (1:1); 4- 0.047 Mn/ZnO (1:1).

in this series (Fig. 8A, curve 4). Therefore we could speak about the existence of a certain threshold, above which the influence of the dopant concentration begins to manifest itself.

The increase of the oxide activity at such low dopant concentrations could be explained with: i) the dopant segregation on the crystal surface in the process of oxalate decomposition, which would lead to an increase in its effective concentration ii) the existence of several oxidation states of manganese. In order to check the first possibility, an X-ray photoelectron spectroscopy investigation was carried out with the 0.151 Mn/ZnO sample, containing the "highest" quantity of Mn (Fig. 9). As it can be seen no signals of Mn ions are observed, but only those of Zn and O. This is an indication that the manganese ions are uniformly distributed in the crystals. There exists a definite minimal concentration on the surface, which still displays a comparatively high catalytic activity.

For determination of the oxidation state of manganese, an EPR investigation of the same 0.151% Mn-ZnO (1:2) sample was carried out (Fig. 10). The result for the sample 0.035 Mn/ZnO from series (1:1) is also represented. It is well known that Mn2+ is used as a standard in the EPR spectroscopy. Mn4+ does not give EPR signal, while Mn3+ gives a wide line, which is not observed in our case. This shows that even if it exists it is only in a minimal amount. Fig. 10 displays a typical signal of 6 lines, which is indicative of two things: manganese is mainly in the form of Mn2+ in the crystal lattice of ZnO and there is no magnetic interaction between the ions (if there was any interaction these six lines could not be obtained). The presence of mainly Mn<sup>2+</sup>, whose magnetic moment is 5.92 BM, was also confirmed by magnetic measurements below 100°C. The presence of Mn<sup>3+</sup> and Mn<sup>4+</sup> would significantly decrease the magnetic moment, but this was not observed. Due to low manganese concentrations the reliability of magnetic

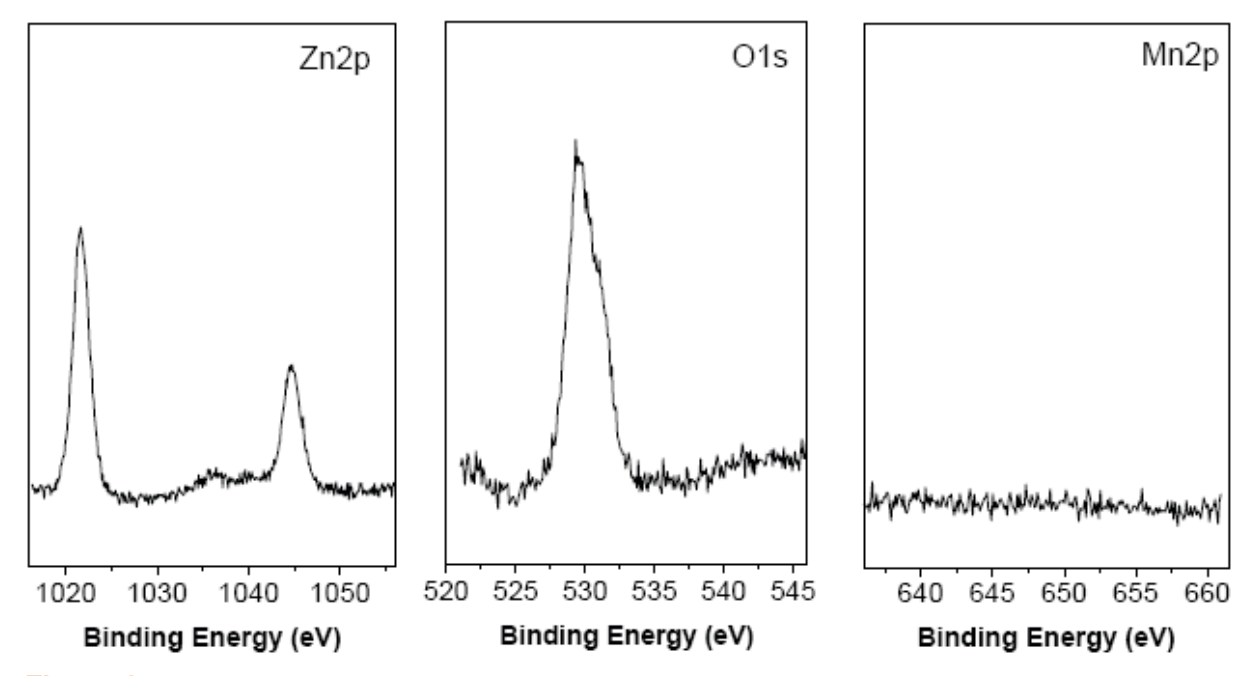


Figure 9. XPS spectra of Zn 2p, O 1s and Mn 2p core levels from the sample 0.151 Mn/ZnO (1:2).

measurements is small, so they can be regarded only as a confirmation of the EPR measurements.

Briefly, the XPS and EPR analyses showed that in our oxides, containing Mn ≤ 0.151 Wt %, the manganese is basically in the +2 oxidation state and it is uniformly distributed in the catalyst without measurable segregation on its surface. Then one can suppose that the reason for the catalytic activity of these low dopant concentrations is the specific way of its incorporation into the support – by co-crystallization during the synthesis process of the precursor and the absence of interaction between the manganese ions. When the manganese becomes involved in a specific catalytically active site of the obtained zinc oxide then a new type of catalytic complex is being formed, displaying a higher catalytic activity.

The catalytic tests revealed another interesting fact - that the catalytic activity depends on the ratio of Zn<sup>2+</sup>:C<sub>2</sub>O<sub>4</sub><sup>2-</sup>. As was mentioned above the catalysts of the 1:2 series are more active than those of the 1:1 series. One of the reasons is the different morphology of the obtained oxides from series 1:1 and 1:2 (see Fig. 4). The investigation of the adsorption capacity of ZnO with respect to CO, CO<sub>2</sub>,H<sub>2</sub> and CO<sub>2</sub>/H<sub>2</sub> adsorption showed that it is increasing with the increase in the number of the so called "polar faces" of the oxide [36]. Probably, the number of these polar faces is bigger in the 1:2 series samples and if their adsorption capacity is higher we suppose that it will result in higher catalytic activity. This difference is not expressed in the non-doped samples, probably due to their low activity.

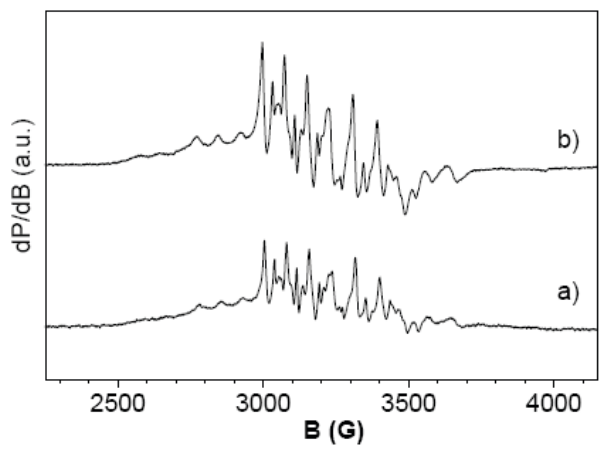


Figure 10. EPR spectra of a) 0.035 Mn/ZnO (1:1); b) 0.151 Mn/ZnO (1:2)

Another reason for the dependence of the activity on the ratio  $Zn^{2+}$ : $C_2O_4^{\ 2-}$  undoubtedly is the different mechanism of Mn inclusion during the precursor synthesis, established in Refs. [21-23]. At a ratio  $Zn^{2+}$ : $C_2O_4^{\ 2-}=1:1$  the manganese cannot form neutral oxalate complexes  $[MnC_2O_4]^o$  (through which the crystalline oxalate phase is growing up) because of the lower stability constant with respect to that of  $[ZnC_2O_4]^o$ . For this reason Mn is slightly included, mainly by participating in the ion exchange with the first subsurface layer (called Panet layer). In case of oxalate ions excess (series 1:2) the manganese forms neutral complexes, whereupon it can participate directly both in the process of crystal formation and in the growth

of the crystalline phase by substituting the zinc neutral complexes in the adsorption layer (Volmer's layer) [21-23]. The expectation is in this way a considerably more uniform distribution in the crystal lattice is achieved, which passes over to the oxide product.

### 4. Confusions

The results show that the initial ratio  $Zn^{2+}:C_2O_4^{2-}=1:1$  and 1:2 exerts influence on the morphology and on the prevailing orientations of the crystallites in the oxalate samples and not only on the quantity of the inserted dopant as established in [21]. This leads to the differences both in the X-ray diffractograms and in the parameters of the crystal lattice. There is a tendency, also, to obtain larger size of product crystallites in the series (1:2). The presence of Mn in the samples does not influence the morphology of the crystals.

After thermal decomposition of the precursors both pure and doped oxide samples are obtained with manganese content  $0.51\times10^{-2}$   $-15.1\times10^{-2}$  Wt %. It is important that the oxides preserved the morphology of the precursors. SEM observation suggests that the micron-sized oxide crystals are obtained as a result of the growth of nanometer-sized particles. After decomposition significant increase of the specific surface area is observed, which is also dependent on the initial ratio of  $Zn^{2+}$ :  $C_2O_4^{-2-}$ .

The catalytic tests show that ZnC<sub>2</sub>O<sub>4</sub>·2H<sub>2</sub>O, doped

#### References

- [1] R. Janisch, P. Gopal, N.A. Spaldin, J. Phys.: Condens.Matter. 17, R657 (2005)
- [2] G.-C. Yi, C. Wang, W.I. Park, Semicond. Sci. Technol. 20, S22 (2005)
- [3] Ü. Özgür et al., J. Appl. Phys. 98, art. 041301 (2005)
- [4] S.J. Pearton et al., Mat. Sci. Eng. R40, 137 (2003)
- [5] In: C. Jagadish, S. Pearton (Eds), Zinc Oxide Bulk, Thin Films and Nanostructures, 1st edition (Elsevier, Oxford, 2006)
- [6] K.G. Kanade, B.B. Kale, R.C. Aiyer, B.K. Das, Mater. Res. Bull. 41, 590 (2006)
- [7] G.M. Duffy, S.C. Pillai, D.E. McCormack, J. Mater. Chem. 17, 181 (2007)
- [8] S.C. Pillai, J.M. Kelly, D.E. McCormack, P. O'Brien, R. Ramesh, J. Mater. Chem. 13, 2586 (2003)
- [9] L. Guo, Y. Ji, H. Xu, Z. Wu, P. Simon, J. Mater. Chem. 13, 754 (2003)
- [10] T. Ahmad, S. Vaidya, N. Sarkar, S. Ghosh, A.K. Ganguli, Nanotechn. 17, 1236 (2006)
- [11] L. Yang, G. Wang, C. Tang, H. Wang, L. Zhang, Chem. Phys. Lett. 409, 337 (2005)

with manganese by co-crystallization, could serve as precursors for doped low-percentage oxide catalysts for the CO oxidation reaction. The pure zinc oxide has a poor catalytic activity. Its doping with manganese promotes the catalytic activity (up from twice to five times) in spite of the very low contents of manganese. This process depends not only on the Mn contents but also mainly on the ratio of Zn 2+: C2O22 . The catalysts of the 1:2 series are slightly more active than those of the 1:1 series, at one and the same specific surface area and quite close in Mn content. It is seen from the XPS data that manganese does not segregate on the surface of the catalyst. The EPR analyses show that the manganese is mainly in the +2 oxidation state, being uniformly distributed in the catalyst. Therefore it should be supposed that the involvement of manganese in a specific catalytic center of the zinc oxide results in a formation of a new type of catalytically active complex (CAC), and this new complex possesses a higher catalytic activity.

# **Acknowledgements**

The authors are thankful to Prof. K. Petrov for interpretation of XRD data, to Assoc. Prof. R. Stoyanova and Assoc. Prof. P. Stefanov for the support about the EPR and XPS analyses. This work has been financially supported by the Scientific Research Fund of Sofia University (Project 020/2007).

- [12] S.C. Pillai, J.M. Kelly, D.E. McCormack, R. Ramesh, J. Mater. Chem. 14, 1572 (2004)
- [13] H. Niu, Q. Yang, K. Tang, Y. Xie, F. Yu, J. Mater. Sci. 41, 5784 (2006)
- [14] C.J. Cong, L. Liao, J.C. Li, L.X. Fan, K.L. Zhang, Nanotechn. 16, 981 (2005)
- [15] C.J. Cong, L. Liao, Q.Y. Liu, J.C. Li, K.L. Zhang, Nanotechn. 17, 1520 (2006)
- [16] S. Thota, T. Dutta, J. Kumar, J. Phys.: Condens. Matter. 18, 2473 (2006)
- [17] W. Doerffler, K. Hauffe, J. Catal. 3(2), 171 (1964)
- [18] G.I. Tcheejeekova, Kin. Cat. 7(4), 666 (1966) (in Russian)
- [19] W. Komatsu, H. Ooki, I. Naka, A. Kobayashi, J. Catal. 15(1), 43 (1969)
- [20] P. Amigues, S.J. Teichner, Discuss. Far. Soc. 41, 362 (1966)
- [21] B. Donkova, J. Pentsheva, M. Djarova, Cryst. Res. Technol. 39(3), 207 (2004)
- [22] J. Pencheva, B. Donkova, M. Djarova, Cryst. Res. Technol. 40, 370 (2005)

- [23] B.V. Donkova, PhD thesis, University of Sofia (Sofia, BG, 2005) (in Bulgarian)
- [24] J.A. Allen, J. Phys. Chem. 57, 715 (1953)
- [25] R. Deyrieux, C. Berro, A. Peneloux, Bull. Soc. Fr. Mineral. Cristallogr. 1, 25 (1973)
- [26] A. Packter, P. Chauhan, Krist. Tech. 10(6), 621 (1975)
- [27] I.V. Melikhov, E. Kirkova, M.D. Djarova, J. Cryst. Growth 53, 547 (1981)
- [28] M. Djarova, M. Tchaneva, J. Cryst. Growth 79, 636 (1986)
- [29] M. Djarova, A.E. Nielsen, Ann. Univ. Sofia, Fac. Chim. 84, 49 (1992)

- [30] V. Kraus, J. Nolze, Powder Cell, version 2.4, (2000).
- [31] C. Pierce, J. Phys. Chem. 57,149 (1953)
- [32] N. Audebrand, J.-P. Auffrédic, D. Louër, Chem. Mater. 10, 2450 (1998)
- [33] D. Dollimore, D. Nicholson, J. Chem. Soc., 908 (1964)
- [34] V. Bolis, B. Fubini, E. Giamello, A. Reller, J. Chem. Soc. Far. Trans. 85(4), 855 (1989)
- [35] IUPAC Recommendation 1984, Pure Appl. Chem. 57, 603 (1985)
- [36] M. Bowker, H. Houghton, K.C. Waugh, T. Giddings, M. Green, J. Catal. 84(1), 252 (1983)